

# Deep CO Observations and the CO-to-H<sub>2</sub> Conversion Factor in DDO 154, a Low Metallicity Dwarf Irregular Galaxy

Shinya KOMUGI<sup>1,2</sup>, Chikako YASUI<sup>2</sup>, Naoto KOBAYASHI<sup>3</sup>, Bunyo HATSUKADE<sup>2</sup> Kotaro KOHNO<sup>3</sup>, Yoshiaki SOFUE<sup>4</sup>

and

Shiori KYU<sup>3</sup>

<sup>1</sup>*Institute of Space and Astronautical Science, Japan Aerospace Exploration Agency,  
3-1-1 Yoshinodai, Sagamihara, Kanagawa, 229-8510*

<sup>2</sup>*National Astronomical Observatory of Japan, 2-21-1 Osawa, Mitaka-shi, Tokyo, 181-8588*

<sup>3</sup>*Institute of Astronomy, The University of Tokyo, 2-21-1 Osawa, Mitaka-shi, Tokyo, 181-8588*

<sup>4</sup>*Dep. Physics, Meisei University, Hino, Tokyo, 191-8506*

*s.komugi@nao.ac.jp*

(Received <reception date>; accepted <acceptation date>)

## Abstract

We present a deep spectroscopic search for CO emission in the dwarf irregular galaxy DDO154, which has an Oxygen abundance of only 1/20 the solar value. The observations were conducted in order to constrain the CO-to-H<sub>2</sub> conversion factor at low metallicity. No CO was detected, however, despite being one of the sensitive observations done towards galaxies of this type. We succeed in putting a strong lower limit on the conversion factor, at least 10 times the Galactic value. Our result supports previous studies which argue for a high conversion factor at low metallicity.

**Key words:** galaxies:ISM — ISM:molecules — stars:formation

## 1. Introduction

Tracing the molecular gas content is an essential part of studying star formation in galaxies. Molecular hydrogen, however, cannot be observed directly except in hot and/or shocked environments because of its lack of dipole moments. Consequently, CO lines have been used via the “CO-to-H<sub>2</sub> conversion factor ( $X_{\text{CO}}$ )” to calibrate the molecular gas quantity. Measurements of  $X_{\text{CO}}$  are conducted mainly by comparing the dynamical mass and the CO luminosity of a molecular cloud, and is known to be constant (but with considerable scatter) in the Milky way at around  $X_{\text{CO}} = 3.0 \times 10^{20} \text{ (cm}^{-2} \text{ (K km s}^{-1} \text{)}^{-1} \text{)}$  (Scoville et al. 1987; Strong

et al. 1988). The value of  $X_{\text{CO}}$  in other environments is controversial, however. In particular, the study of  $X_{\text{CO}}$  and its dependence on metallicity in low metallicity environments have met severe difficulties. While Wilson (1995) and Arimoto et al. (1996) find an increasing  $X_{\text{CO}}$  with decreasing metallicity, Rosolowsky et al. (2003), Bolatto et al. (2004), Bolatto et al. (2008) and others find a constant value of  $X_{\text{CO}}$  within a range of metallicities. It is important to note, however, that previous studies which find a constant conversion factor are based on CO observations at relatively high metallicities, i.e., higher than  $12 + \log[\text{O}/\text{H}] \sim 8.0$ . In order to gain decisive information on the metallicity dependence of  $X_{\text{CO}}$ , observations at low metallicities is necessary. This has been a difficult task, however, because CO has failed to be detected in galaxies with metallicity lower than  $12 + \log[\text{O}/\text{H}] \sim 8.0$  (Taylor & Klein 2001; Leroy et al. 2005). The lowest metallicity galaxy with detected CO is IZw 36, at  $12 + \log[\text{O}/\text{H}] \sim 7.9$  Young et al. 1995 which is only tentative. Attempts to detect CO in low metallicity systems (Ohta et al. 1988; Wilson 1992; Ohta et al. 1993; Verter & Hodge 1995; Taylor & Klein 2001; Buyle et al. 2006) may have failed for two reasons; 1) CO fails to be a good tracer of molecular gas at such metallicities (i.e., a high conversion factor), or 2) Molecular gas is actually less abundant in such galaxies. While the first explanation is supported from theoretical views (Maloney & Black 1988; Sakamoto 1996; Bell et al. 2006), the second explanation is less convincing, since star formation is still found in low metallicity dwarfs, and star formation requires gas at high densities.

In either case, calibrating  $X_{\text{CO}}$  requires an actual detection of CO in these low metallicity systems. We have conducted a deep search for  $^{12}\text{CO}(J = 1 - 0)$  in the low metallicity dwarf irregular galaxy DDO 154, a member of the Local Group.

Section 2 explains the target galaxy and the observed region. Section 3 presents observations at the Nobeyama Radio Observatory (NRO) 45m telescope and the Institut Radio Astronomie Millimetrique (IRAM) 30m telescope, and the resulting spectra. Section 4 discusses the  $X_{\text{CO}}$ , and its upper limits.

## 2. Observing Target

### 2.1. DDO 154

DDO154 is a low surface brightness (LSB) dwarf irregular (dI) galaxy located at a distance of 3.2 Mpc (Carignan & Purton 1998:CP98), with an optical radius of  $R_{Ho} = 1.4\text{kpc}$ . The metallicity of  $12 + \log[\text{O}/\text{H}] = 7.67$  (van Zee et al. 1997, Kennicutt & Skillman 2001; KS01), which is about 1/20 of our Galaxy, places DDO154 as one of the most metal-deficient galaxies. Basic properties of DDO 154 are presented in table 1. DDO154 is unique in that dark matter constitutes 90% of its dynamical mass, therefore giving it the name “dark galaxy” (Kennicutt & Skillman 2001). Stars account for only 2% of the dynamical mass, with  $M_{\text{HI}}/L_B = 8$ , and  $M_{\text{HI}} = 2.5 \times 10^8 M_{\odot}$  (Carignan & Beaulieu 1989), placing DDO154 one of the most gas rich

**Table 1.** Properties of DDO 154 and Region 2

DDO 154		Ref.
R.A.(J2000)	12 54 05.2	(1)
Dec.(J2000)	27 08 59	(1)
Morphology	IB(s)m	(1)
Distance	3.2 Mpc	(2)
Optical Radius	1.4 kpc	(2)
$V_{\text{rad}}$	$374 \text{ km s}^{-1}$	(1)
$12 + \log(O/H)$	7.67	(3)
$M_{\text{HI}}$	$2.5 \times 10^8 M_{\odot}$	(2)
$L_B$	$3.1 \times 10^7 L_{\odot}$	(2)
Region 2		
R.A.(J2000)	12 54 03.9	(4)
Dec.(J2000)	27 09 05	(4)
$L(\text{H}\alpha)$	$7.0 \times 10^{36} \text{ (erg s}^{-1}\text{)}$	(4)
Radius	$3.5''$	(4)

References; (1) From the NASA Extragalactic Database (NED). (2) Carignan & Purton (1998). (3) van Zee et al. (1997). (4) Kennicutt & Skillman (2001).

galaxies known. Spectroscopy by KS01 reveals that its oxygen yield is consistent with a closed box model, making it a candidate for one of the most unevolved Population I systems. Star formation is evident from  $\text{H}\alpha$  observations. Sixteen HII regions were identified in KS01, and the ratio of the present star formation rate to average past star formation rate (birthrate parameter  $b$ ) was found to be 1/2 to 1/3, showing a quiescent phase. The gas consumption time is found to be over 200 Gyr (Kennicutt & Skillman 2001).

The richness of neutral gas compared to any other previously observed low metallicity sources, and the presence of substantial star formation requiring an ample amount of molecular gas, make DDO154 the optimum target for detecting CO in a low metallicity environment.

## 2.2. Region 2

Of the HII regions identified in KS01, we selected Region 2 as our target for the CO emission search. Figure 1 shows the  $24\mu\text{m}$ ,  $\text{H}\alpha$  (KS01) and HST F606W band image. Various properties of Region 2 are presented in table 1.

Region 2 is a relatively compact HII region with a diameter of  $7''$ , corresponding to 110 pc (KS01). The  $\text{H}\alpha$  luminosity of  $L(\text{H}\alpha) = 7.0 \times 10^{36}$  is the third most luminous as a single discrete HII region, and the brightest of those with deep spectroscopy by KS01. This luminosity corresponds to a star formation rate of  $1.0 \times 10^{-3} M_{\odot} \text{ kpc}^{-2} \text{ yr}^{-1}$ , calculated from the formulation of Kennicutt (1998). Assuming the same star formation law as low surface bright-

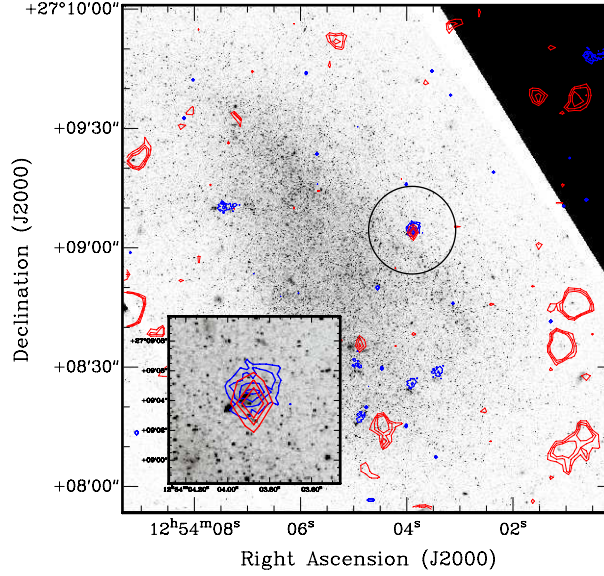


**Fig. 1.**  $H\alpha$  (Blue) and Spitzer MIPS  $24\mu\text{m}$  (Red) contours overlaid on HST F606W image. Region 2 is marked by the black circle, representing the IRAM 30m beamsize of  $22''$ . The inset is a close-up of region 2.

ness galaxies in the same star formation rate range (Bigiel et al. 2008), this star formation rate corresponds to a molecular gas surface density of about  $N(\text{H}_2) \sim 2.5 M_\odot \text{pc}^{-2} = 1.6 \times 10^{20} \text{ cm}^{-2}$ . Absorption of  $H\alpha$  photons by dust can be neglected here, based on the following estimate. From the SINGs survey (Kennicutt et al. 2003) data release 5, the  $24\mu\text{m}$  luminosity of Region 2 is  $\nu L(24) = 7.2 \times 10^{22} \text{ (erg s}^{-1}\text{)}$ . Assuming that the scaling between  $H\alpha$  and  $24\mu\text{m}$ -derived star formation rates can be approximated as in Calzetti et al. (2007), the  $24\mu\text{m}$  contribution to the true star formation rate is only  $\sim 3\%$ . This is in accordance with the low logarithmic  $H\beta$  extinction derived by Kennicutt & Skillman (2001) of  $C(H\beta) = 0.0$ .

The negligible dust extinction may seem inconsistent with the  $24\mu\text{m}$  emission and the assumed presence of molecular gas, but the ISM generally has a clumpy geometry as observed routinely in the Milky Way and other nearby galaxies (Bally et al. 1987). It is probable that dust has a clumpy distribution around Region 2, so that most sightlines toward the HII region are extinction-free, but that most of the molecular gas is confined in a small fraction of the area hidden by high density dust.

HST observation (see figure 1 inset) reveals an apparently associated stellar cluster in this region. Further, Region 2 is the only source in this galaxy that is detected both at  $24\mu\text{m}$  and  $H\alpha$ , suggesting that this source is a candidate for the youngest cluster in DDO 154, with ample molecular gas.

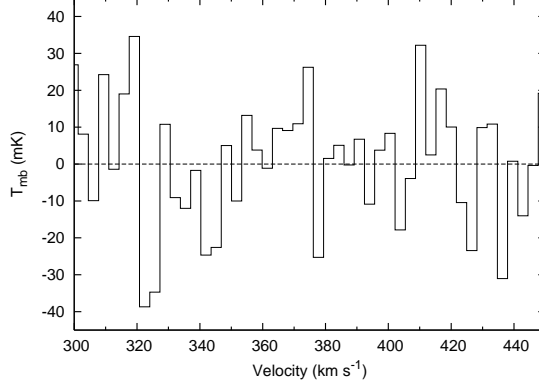


**Fig. 2.** Spectrum of Region 2 from the NRO 45m telescope. Only the velocity range in the vicinity of Region 2 is shown.

### 3. Observation

#### 3.1. NRO 45m

The  $^{12}\text{CO}(J = 1 - 0)$  line (rest frequency 115.271204 GHz) was observed with the Nobeyama Radio Observatory (NRO) 45m telescope in April, 2007. Two SIS receivers, S100 and/or S80, were used for the observations. The backend was the 2048 channel acousto-optical spectrometer (AOS) with a frequency resolution of 250MHz, centered at the systemic velocity of DDO 154, 374  $\text{km s}^{-1}$ . The CO line was observed in the upper sideband. Calibration was done with the standard chopper-wheel method. Typical system temperatures ranged from 700 to 1000 K, under relatively bad weather conditions. Approximately 20 hours were spent on source.

The beamwidth was 15'' at 115.3 GHz. Pointing accuracy was checked using SiO masers or a continuum source (3C273) at 43GHz every 1.5-2 hours, and found to be accurate within 8'' during most of the run.

The obtained data were reduced with the NEWSTAR software used commonly at NRO, which is based on the AIPS package. After flagging of bad spectra, a first order baseline was subtracted and then averaged. The antenna temperature  $T_A^*$  was converted to main beam temperature  $T_{\text{mb}}$  through  $T_A^* = \eta_{\text{eff}} T_{\text{mb}}$  where  $\eta_{\text{eff}}$  is the main beam efficiency, taken to be 0.34 based on December 2006 observations of the Saturn and 3C279.

After binning the resulting spectrum to 3.3 km/s resolution,  $1\sigma$  r.m.s noise was 17 mK ( $T_{\text{mb}}$ ; 5.8mK in  $T_a^*$ ). The spectrum is shown in figure 2.

No signal was detected, and we therefore conducted further follow-up observations at the Institut de Radio Astronomie Millimetrique (IRAM) 30m telescope.

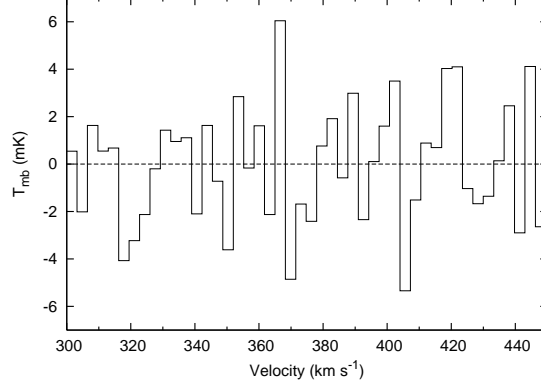


**Fig. 3.** Spectrum of Region 2 from the IRAM 30m telescope. Only the velocity range in the vicinity of Region 2 is shown.

### 3.2. IRAM 30m

The  $^{12}\text{CO}(J = 1 - 0)$  line (rest frequency 115.271204GHz) was observed with the IRAM 30m telescope in November, 2007. Two SIS receivers, A100 and B100, were used in combination with the VESPA spectrometer. The typical system temperature was 320 K. Approximately 5 hours were spent on source. The beamwidth at 115 GHz is  $22''$ .

The obtained data were reduced with the CLASS software. After flagging of bad spectra, a second order baseline was subtracted and then averaged. The main beam efficiency  $\eta_{\text{eff}}$  was taken to be 0.7, based on March 2005 observation of Mars and Uranus. The spectrum was binned to give a final velocity resolution of 3.3 km/s. The  $1\sigma$  r.m.s. noise was 2.6 mK ( $T_{\text{mb}}$ ). The spectrum is shown in figure 3.

No signals were detected above the  $3\sigma$  threshold. The  $3\sigma$  upper limit for the CO intensity can be calculated by

$$I_{\text{CO}} < 3\sigma_{\text{rms}}\sqrt{\delta V \Delta V_{\text{CO}}} \quad [\text{K km s}^{-1}] \quad (1)$$

where  $\sigma_{\text{rms}}$  is the r.m.s. noise at a velocity resolution  $\delta V$  of 3.3 km/s,  $\Delta V_{\text{CO}}$  the line width. Since the CO line was not detected,  $\Delta V_{\text{CO}}$  is a free parameter. Using the measurements obtained at IRAM 30m, we obtain

$$I_{\text{CO}} < 0.014\sqrt{\Delta V_{\text{CO}}}. \quad (2)$$

## 4. Discussion

A relation between molecular cloud size and CO line width exists for Galactic molecular clouds (Dame et al. 1986; Solomon et al. 1987) and also in lower metallicity environments like the LMC (Mizuno et al. 2001) and NGC6822 (Gratier et al. 2010). Assuming that the same relation applies to molecular clouds in DDO154, the size of the observed HII region ( $\sim 100$  pc) gives an upper limit on the line width  $\Delta V_{\text{CO}}$  of 10 km/s. Substituting this value to equation (2)

gives  $I_{\text{CO}} < 0.05$ . This upper limit is the smallest yet obtained for any low metallicity galaxy (figure 4).

We use this upper limit in the discussions that follow. This intensity estimate should be robust, considering that molecular gas is unlikely extended as much as the HII region itself; the dust seen at  $24\mu\text{m}$  is unresolved, where the MIPS  $24\mu\text{m}$  resolution of  $6''$  corresponds to  $\sim 90$  parsec.

Using the value above and the estimated column density of  $\Sigma_{\text{H}_2} = 1.6 \times 10^{20} \text{ cm}^{-2}$  from section 2.2, we obtain a lower limit on the CO-to- $\text{H}_2$  conversion factor of

$$\frac{X_{\text{CO}}}{[\text{cm}^{-2} (\text{K km s}^{-1})^{-1}]} = \frac{N(\text{H}_2) [\text{K km s}^{-1}]}{[\text{cm}^{-2}] I_{\text{CO}}} > 3.1 \times 10^{21} \quad (3)$$

which is  $\sim 10$  times the Galactic value.

Alternative to the gas column density estimation used here which is based on the Schmidt-Kennicutt type relation (e.g., Kennicutt 1998, Komugi et al. 2005), we may estimate the gas column density via a more local argument as done in Verter & Hodge (1995) and Taylor & Klein (2001):

$$\frac{N(\text{H}_2)}{[\text{cm}^{-2}]} = 9.5 \times 10^{-23} \frac{L(\text{H}\alpha) (\text{erg s}^{-1}) \tau_{\text{SF}} (\text{yr})}{\epsilon_{\text{SF}} R (\text{pc})^2} \quad (4)$$

where  $\tau_{\text{SF}}$ ,  $\epsilon_{\text{SF}}$ , and  $R$  are the timescale of star formation, star formation efficiency, and radius of the molecular cloud, respectively. Collisions between clouds can regulate  $\tau_{\text{SF}}$  (Komugi et al. 2006), and the upper limit on the cloud collision timescale can be estimated by the crossing time (Lo et al. 1993), which is often applied in local star formation arguments as done here (Verter & Hodge 1995; Taylor & Klein 2001). In DDO154, the rotation velocity of  $\sim 30 \text{ km s}^{-1}$  at the optical radius of 1.4 kpc (Carignan & Beaulieu 1989) sets  $\tau_{\text{SF}} \leq 2 \times 10^8 \text{ yr}$ . The lower limit of  $\tau_{\text{SF}}$  is constrained by the timescale of disruption by OB stars, which is  $\text{few} \times 10^7 \text{ yr}$  in nearby galaxies (e.g., Egusa et al. 2004, Egusa et al. 2009). We therefore assume  $\tau_{\text{SF}} = 10^8 \text{ yr}$ , in accordance with previous studies. For  $\epsilon_{\text{SF}}$ , it has been known that the overall star formation efficiency of clusters is few - 30% in the solar neighborhood, with a tendency for lower  $\epsilon_{\text{SF}}$  in less evolved, young clusters (Lada & Lada 2003). For entire molecular clouds,  $\epsilon_{\text{SF}}$  is observed to be lower than 10% in our Galaxy (e.g., Duerr et al. 1982, Evans & Lada 1991) and also in nearby galaxies (Wilson & Matthews 1995; Taylor et al. 1999). Even in low metallicity systems which may have higher star formation efficiencies,  $\epsilon_{\text{SF}} = 0.2$  should give a conservative upper limit estimate (e.g., Yasui et al. 2008). Substituting these values and the molecular cloud radius upper limit of  $R = 50$  parsecs into equation (4), we obtain  $N(\text{H}_2) > 1.4 \times 10^{20}$  and a corresponding lower limit of  $X_{\text{CO}} > 2.7 \times 10^{21}$ . Although this estimate is highly uncertain considering large uncertainties in  $\tau_{\text{SF}}$  and  $\epsilon_{\text{SF}}$ , and accurate to factors of few at best, the  $X_{\text{CO}}$  lower limit obtained using two different methods, the former based on an empirical global star formation law and the latter based on local star formation processes, are consistent at  $\sim 10$  times larger than the typical Galactic value. The lower limit on the conversion factor



is consistent with the  $X_{\text{CO}}$ -metallicity relation, as shown by Wilson 1995 and Arimoto et al. 1996. Our results, however, are inconsistent with constant conversion factor as a function of metallicity, as claimed by Rosolowsky et al. 2003, Bolatto et al. 2004; Bolatto et al. 2008, which is valid only above  $12 + \log[\text{O}/\text{H}] \sim 8.0$ .

In order for our CO intensity upper limit to be consistent with a Galactic conversion factor, increasing the star formation efficiency  $\epsilon_{\text{SF}}$  to 1 is not sufficient. The star formation timescale  $\tau_{\text{SF}}$  must also become significantly shorter, so that the molecular cloud converts all of its gas into stars in at most several times  $10^7$  years, which seems difficult to realize.

It should be pointed out that our observation is done towards a single star forming region, which is unresolved by the telescope beam. The strong UV radiation field from the central stars in a metal-poor environment should make the CO emitting region smaller (Maloney & Black 1988), so that the molecular gas is distributed in a more extended way than the CO molecules. The Schmidt-Kennicutt law estimation of molecular gas implicitly derives the total molecular gas surface density within the unresolved region, including diffuse molecular gas that is not directly associated with Region 2. Therefore, the  $X_{\text{CO}}$  estimation given here may still be biased towards a higher value as pointed out in Wilson 1995. In order to mitigate such biases, we have stressed the selection of conservative values whenever possible. The consistent lower limit on  $X_{\text{CO}}$  given from molecular gas estimation based on a individual molecular gas argument in equation (4), may justify the use of such methods using an empirical star formation law. Nevertheless, figure 4 alone should not be taken as an indication on  $X_{\text{CO}}$  at low metallicities, but as a representation of how CO is undetectable at such metallicities, and the depth of the CO observation given here.

## 5. Summary and Conclusions

We have obtained sensitive spectra in search of CO in DDO154, a low metallicity dwarf irregular galaxy. In particular, the targeted HII region (Region 2) is expected to contain a detectable amount of molecular gas, if a Galactic conversion factor is applicable in such low metallicity environments. Using two large aperture single dish telescopes, however, we did not detect any significant CO emission in Region 2.

The obtained upper limit on the CO intensity is one of the lowest in a low metallicity dwarf galaxies. We calculate the expected molecular column density from two views, one based on the Schmidt-Kennicutt law extrapolated to low densities, and another based on a local argument of a collapsing molecular cloud. Both estimations gave similar values. Applying a method used previously (e.g., Verter & Hodge 1995) and using conservative values in all assumptions, we derive a lower limit on the CO-to- $\text{H}_2$  conversion factor which is at least 10 times higher than in the Milky Way. Our results strongly support a an increasing conversion factor with decreasing metallicity, but inconsistent with a constant (Galactic) conversion factor, unless the molecular cloud forms stars very efficiently (all of the gas converted to stars)



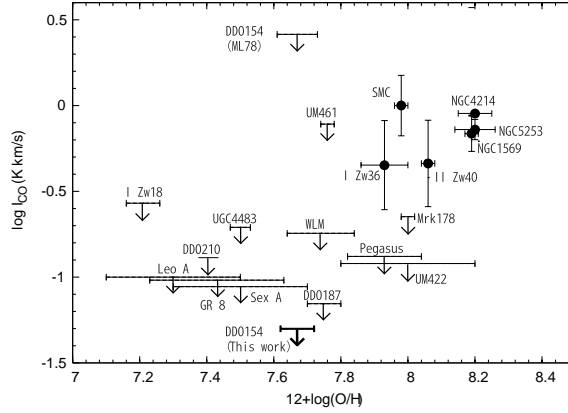


**Fig. 4.** Previous observations of CO in low-metallicity dwarfs. Our  $3\sigma$  upper limit on the CO intensity of DDO 154 is shown by the bold arrow. The metallicity and CO intensities are taken from Pagel et al. (1978), Israel et al. (1993), Young et al. (1995), Kobulnicky & Skillman (1996), Kobulnicky & Skillman (1997), Kobulnicky et al. (1997), Viallefond & Thuan (1983), Skillman & Kennicutt (1993), Gallagher et al. (1998), van Zee et al. (1997), Morris & Lo (1978):ML78, Sage et al. (1992), Terlevich et al. (1991), Skillman et al. (1988), Skillman et al. (1989), Skillman et al. (1994), Skillman et al. (1997), and Taylor et al. (1998), following figure 2 in Taylor et al. (1998). For the previous DDO154 observation by ML78, only the  $3\sigma$  upper limit in antenna temperature  $T_a$  is given at 2.6 km/s velocity resolution; we converted it to intensity using an antenna efficiency of 0.5 and velocity width of 10 km/s.

at a timescale significantly shorter than  $10^8$  years. Molecular gas masses in ultra-low metallicity systems estimated using Galactic conversion factors may underestimate masses significantly.

S.K. is grateful to the staffs at the NRO and IRAM, for their generous support in the observations. S.K. thanks N. Sakai for suggestions on data reduction. We acknowledge the usage of the NASA/IPAC Extragalactic Database (NED), which is operated by the Jet Propulsion Laboratory, Caltech, under contract with the National Aeronautics and Space Administration. S.K., C.Y., and B.H. were supported by the Research Fellowship from the Japan Society for the Promotion of Science for Young Scientists.

## References

- Arimoto, N., Sofue, Y., & Tsujimoto, T. 1996, PASJ, 48, 275
- Bally, J., Lanber, W. D., Stark, A. A., & Wilson, R. W. 1987, ApJL, 312, L45
- Bell, T. A., Roueff, E., Viti, S., & Williams, D. A. 2006, MNRAS, 371, 1865
- Bigiel, F., Leroy, A., Walter, F., Brinks, E., de Blok, W. J. G., Madore, B., & Thornley, M. D. 2008, AJ, 136, 2846
- Bolatto, A. D., Leroy, A., Simon, J. D., Blitz, L., & Walter, F. 2004, The Dense Interstellar Medium in Galaxies, 155
- Bolatto, A. D., Leroy, A. K., Rosolowsky, E., Walter, F., & Blitz, L. 2008, ApJ, 686, 948

- Buyle, P., Michielsen, D., de Rijcke, S., Ott, J., & Dejonghe, H. 2006, *MNRAS*, 373, 793  
 Calzetti, D., et al. 2007, *ApJ*, 666, 870  
 Carignan, C., & Beaulieu, S. 1989, *ApJ*, 347, 760  
 Carignan, C., & Purton, C. 1998, *ApJ*, 506, 125  
 Dame, T. M., Elmegreen, B. G., Cohen, R. S., & Thaddeus, P. 1986, *ApJ*, 305, 892  
 Duerr, R., Imhoff, C. L., & Lada, C. J. 1982, *ApJ*, 261, 135  
 Egusa, F., Kohno, K., Sofue, Y., Nakanishi, H., & Komugi, S. 2009, *ApJ*, 697, 1870  
 Egusa, F., Sofue, Y., & Nakanishi, H. 2004, *PASJ*, 56, L45  
 Evans, N. J., II, & Lada, E. A. 1991, *Fragmentation of Molecular Clouds and Star Formation*, 147, 293  
 Gallagher, J. S., Tolstoy, E., Dohm-Palmer, R. C., Skillman, E. D., Cole, A. A., Hoessel, J. G., Saha, A., & Mateo, M. 1998, *AJ*, 115, 1869  
 Gratier, P., Braine, J., Rodriguez-Fernandez, N. J., Israel, F. P., Schuster, K. F., Brouillet, N., & Gardan, E. 2010, *arXiv:1001.5405*  
 Israel, F. P., et al. 1993, *A&A*, 276, 25  
 Kennicutt, R. C., Jr. 1998, *ApJ*, 498, 541  
 Kennicutt, R. C., Jr., & Skillman, E. D. 2001, *AJ*, 121, 1461  
 Kennicutt, R. C., Jr., et al. 2003, *PASP*, 115, 928  
 Kobulnicky, H. A., & Skillman, E. D. 1996, *ApJ*, 471, 211  
 Kobulnicky, H. A., & Skillman, E. D. 1997, *ApJ*, 489, 636  
 Kobulnicky, H. A., Skillman, E. D., Roy, J.-R., Walsh, J. R., & Rosa, M. R. 1997, *ApJ*, 477, 679  
 Komugi, S., Sofue, Y., & Egusa, F. 2006, *PASJ*, 58, 793  
 Komugi, S., Sofue, Y., Nakanishi, H., Onodera, S., & Egusa, F. 2005, *PASJ*, 57, 733  
 Lada, C. J., & Lada, E. A. 2003, *ARA&A*, 41, 57  
 Leroy, A., Bolatto, A. D., Simon, J. D., & Blitz, L. 2005, *ApJ*, 625, 763  
 Lo, K. Y., Sargent, W. L. W., & Young, K. 1993, *AJ*, 106, 507  
 Maloney, P., & Black, J. H. 1988, *ApJ*, 325, 389  
 Mizuno, N., et al. 2001, *PASJ*, 53, 971  
 Morris, M., & Lo, K. Y. 1978, *ApJ*, 223, 803  
 Ohta, K., Sasaki, M., & Saito, M. 1988, *PASJ*, 40, 653  
 Ohta, K., Tomita, A., Saito, M., Sasaki, M., & Nakai, N. 1993, *PASJ*, 45, L21  
 Pagel, B. E. J., Edmunds, M. G., Fosbury, R. A. E., & Webster, B. L. 1978, *MNRAS*, 184, 569  
 Rosolowsky, E., Engargiola, G., Plambeck, R., & Blitz, L. 2003, *ApJ*, 599, 258  
 Sage, L. J., Salzer, J. J., Loose, H.-H., & Henkel, C. 1992, *A&A*, 265, 19  
 Sakamoto, S. 1996, *ApJ*, 462, 215  
 Scoville, N. Z., Yun, M. S., Sanders, D. B., Clemens, D. P., & Waller, W. H. 1987, *ApJS*, 63, 821  
 Skillman, E. D., Bomans, D. J., & Kobulnicky, H. A. 1997, *ApJ*, 474, 205  
 Skillman, E. D., Televich, R. J., Kennicutt, R. C., Jr., Garnett, D. R., & Terlevich, E. 1994, *ApJ*, 431, 172  
 Skillman, E. D., & Kennicutt, R. C., Jr. 1993, *ApJ*, 411, 655  
 Skillman, E. D., Kennicutt, R. C., & Hodge, P. W. 1989, *ApJ*, 347, 875

Skillman, E. D., Terlevich, R., Teuben, P. J., & van Woerden, H. 1988, *A&A*, 198, 33  
 Solomon, P. M., Rivolo, A. R., Barrett, J., & Yahil, A. 1987, *ApJ*, 319, 730  
 Strong, A. W., et al. 1988, *A&A*, 207, 1  
 Taylor, C. L., Kobulnicky, H. A., & Skillman, E. D. 1998, *AJ*, 116, 2746  
 Taylor, C. L., Hüttemeister, S., Klein, U., & Greve, A. 1999, *A&A*, 349, 424  
 Taylor, C. L., & Klein, U. 2001, *A&A*, 366, 811  
 Terlevich, R., Melnick, J., Masegosa, J., Moles, M., & Copetti, M. V. F. 1991, *A&AS*, 91, 285  
 van Zee, L., Haynes, M. P., & Salzer, J. J. 1997, *AJ*, 114, 2479  
 Verter, F., & Hodge, P. 1995, *ApJ*, 446, 616  
 Viallefond, F., & Thuan, T. X. 1983, *ApJ*, 269, 444  
 Wilson, C. D. 1992, *ApJ*, 391, 144  
 Wilson, C. D. 1995, *ApJL*, 448, L97  
 Wilson, C. D., & Matthews, B. C. 1995, *ApJ*, 455, 125  
 Yasui, C., Kobayashi, N., Tokunaga, A. T., Terada, H., & Saito, M. 2008, *ApJ*, 675, 443  
 Young, J. S., et al. 1995, *ApJS*, 98, 219